Linearized waveform inversion with (small) velocity updates

Alejandro Cabrales-Vargas, Biondo Biondi, and Robert Clapp

ABSTRACT

Current implementations of linearized waveform inversion rely on an optimum background model, and only allow updates in the short wavenumber component, *a.k.a.* reflectivity. We attempt to take one step further allowing controlled perturbations in the background model. We propose constraining such perturbations in such a way that we maximize the stacking power, therefore improving even more the estimated reflectivity.
In this report we introduce theoretical insight about what we have called *linearize waveform inversion with velocity update*.

INTRODUCTION

Reverse-time migration (RTM) (Baysal et al., 1983; Kosloff and Baysal, 1983; Gazdag and Carrizo, 1986; McMechan, 1983) constitutes nowadays the best available technique to obtain images of the subsurface for petroleum exploration purposes. In structurally complex areas, RTM has proved its superiority above the most sophisticated implementations of one-way wave equation migration that flourished since the early 90s (e.g. Stoffa et al., 1990; Ristow and Rühl, 1994; Biondi, 2002), when RTM was computationally unaffordable. Such one-way wave equation techniques aimed at solving increasingly steep dips. On the other hand, RTM is based on the two-way wave equation solution, which naturally accounts not only for 90° dips and beyond, but also for wavepath trajectories difficult, if not impossible, to recover with the one-way wave equation, such as prismatic waves, and even multiples (e.g. Liu et al., 2011a, 2015; Wong et al., 2015).

There are, however, some numerical issues associated with the implementation of RTM. The well known crosscorrelation imaging condition (Claerbout, 1971) produces low-wavenumber artifacts that contaminate the image, mainly in the presence of strong velocity contrasts such as sediment-salt interfaces. Such artifacts arise from crosscorrelations of the source and the receiver wavefields components propagating in same directions, whereas the desired solution (corresponding to seismic reflections) is made of corresponding wavefield components propagating in opposite directions. Conventional high-pass filters are not capable of attenuating such noise without harming the image. Proposed solutions consist of simple Laplacian low-cut filters, wavefield separation (Liu et al., 2011b), and Poynting vectors (Yoon and Marfurt, 2006; Ren

et al., 2013; Araujo et al., 2014). Another interesting approach was suggested by Douma et al. (2010), who demonstrated that recasting the imaging conditions using the impedance sensitivity kernel is equivalent to conventional imaging conditions followed by the Laplacian filter. Hence, such technique intrinsically boosts the high-wavenumber components of the image. An equivalent reasoning was proposed by Rocha et al. (2015a,b), through the so-called the energy norm imaging conditions. Such solution allows the attenuation of direct waves, headwaves, and backscattering, which are the main cause of the low-wavenumber artifacts.

Another, rather intrinsical RTM limitation (as a matter of fact, of *any* kind of migration) is that it constitutes the first approximation to the inverse of the seismic modeling experiment, the so-called *adjoint* operator (Claerbout, 2014). As a consequence, conventional migration typically suffers of degradation in resolution and incorrect seismic amplitudes. This situation has encouraged intense research in inversion schemes aimed at obtaining more realistic estimations of the subsurface reflectivity. One product of such research is *linearized waveform inversion* (LWI), more commonly known as least-squares migration (e.g. Nemeth et al., 1999; Duquet et al., 2000; Ronen and Liner, 2000; Jiang and Schuster, 2003). This procedure consists of minimizing a scalar function that quantifies the mismatch between synthetic data and recorded data. Synthetic datasets are produced by applying the *Born modeling approximation* to reflectivity models of the subsurface. Ideally, we would search for the reflectivity model that corresponds to the minimum value of the mismatch function. The optimization can be performed in the data space or in the model space, iteratively updating the reflectivity with the aid of optimization methods such as steepest descent or conjugate gradients (Hestenes and Stiefel, 1952). In the data space the procedure requires both the modeling operator and its adjoint. Such operators are constituted by the Born modeling operator (or alternatively, one demigration operator), and the RTM operator, respectively. In the model space we apply the *Hessian* operator, that can be constructed applying the modeling operator followed by the adjoint operator to "spiky" perturbations in the model space. In both schemes it is often necessary to include constraints in order to reject solutions corresponding either to the model null space, or to overfitting undesired aspects of the data (e.g. unphysical events such as noise, or propagation modes not accounted for by our modeling and adjoint operators). In the data space every iteration of LWI costs somewhat more than two conventional migrations. Not surprisingly, the first LWI experiments were carried out using comparatively cheaper Kirchhoff-based modeling (or demigration) and migration algorithms. Only after RTM itself became affordable did least-squares RTM (LSRTM) become subject of intense research (e.g. Ji, 2009; Dai et al., 2010; Wong et al., 2011, among many others), although the original idea can be traced back many years earlier (Ji, 1992). In order to tackle the intense computational burden demanded by LSRTM, some techniques have been proposed such as source blending and target oriented methods (Dai et al., 2013). Another relatively recent line of research, instead of relying on traditional amplitude-matched-based LWI, is based on the maximization of the correlation energy at zero lag , and is known as *correlative least-squares RTM* (Zhan et al., 2015). The advantage of such technique is that phase

matching does not require similar amplitudes between observed data and modeled data, which are often difficult to match.

So far, LWI methods aim at improving the reflectivity estimation assuming that the model parameters are optimum. Therefore, our motivation for this report is envisioning an algorithm capable of performing LWI including a controlled velocity perturbation. Such velocity perturbations are expected to be rather small to deserve their incorporation into the velocity model, but significant enough to promote the improvement of the image by maximizing the stacking power. The conception of the method is a linear optimization scheme that updates two different aspects of the model: a perturbation on the low-wavenumber component (related to background velocity) and a perturbation on the high-wavenumber component (related to reflectivity). Thereby, this procedure has different objective than full-waveform inversion (FWI), which is built upon a non-linear optimization scheme that updates the model parameters as one single entity.

This report is organized in three sections. We first make a brief review about basic concepts of LWI and FWI. We then introduce two algorithms to implement LWI with velocity updates. Then we compare the methods and discuss potential advantages and disadvantages, including plausible strategies for practical implementation.

LINEARIZED WAVEFORM INVERSION VS. FULL WAVEFORM INVERSION

In this section we offer a brief discussion about the differences between LWI and FWI in a tutorial style.

Following the notation convention proposed by Barnier and Almomin (2014) we characterize the subsurface by means of elastic parameters (e.g. slowness, density) encompassed by the real variable $\mathbf{m}$. We can split such variable in low-wavenumber and high-wavenumber components:

$$\mathbf{m} = \mathbf{b} + \mathbf{r}, \tag{1}$$

which can be individually perturbed (Barnier and Almomin, 2014),

$$\mathbf{m} = \mathbf{b_0} + \mathbf{\Delta b} + \mathbf{r_0} + \mathbf{\Delta r}, \tag{2}$$

Full waveform inversion performs the minimization of the so-called misfit function, Φ_{FWI}, which quantifies the mismatch between the recorded data, $\mathbf{d}_r$, and the modeled data, $\mathbf{d} = \mathcal{L}(\mathbf{m})$, in the least-squares sense:

$$\Phi_{FWI}(\mathbf{m}) = \|\mathcal{L}(\mathbf{m}) - \mathbf{d_r}\|_{\mathbf{2}}^{\mathbf{2}}. \tag{3}$$

Here $\mathcal{L}(\mathbf{m})$ represents the full wave propagation operator. In the case of a constant-density acoustic medium, $\mathbf{m}$ usually represent the slowness squared, thereby $\mathcal{L}(\mathbf{m})$ is

given as

$$\pounds(\mathbf{m}) : \begin{cases} \left[\mathbf{m}\dfrac{\partial^2}{\partial t^2} - \nabla^2\right]\mathbf{u}(\mathbf{x},t) = \mathbf{s}(\mathbf{x},t) \\ \mathbf{d}(\mathbf{x}_r,t) = \mathbf{u}(\mathbf{x}=\mathbf{x}_r,t) \end{cases} \tag{4}$$

The first term of Equation 4 represents the solution of the acoustic wave equation in a subsurface medium characterized by the slowness squared function $\mathbf{m}$, which constitutes the model parameter. The second term represents the wavefield sampled at the receivers positions. The subsurface medium is excited by external forces represented by the source function $\mathbf{s}(\mathbf{x},t)$.

The operator $\pounds(\mathbf{m})$ is non-linear respect to $\mathbf{m}$, but it is linear respect to the source function, $\mathbf{s}(\mathbf{x},t)$, and respect to the wavefield, $\mathbf{u}(\mathbf{x},t)$. As consequence, one can "decouple" the operator from $\mathbf{u}$ and $\mathbf{s}$, but not from $\mathbf{m}$, which is what we want to invert for. Hence, because of such non-linearity the FWI misfit function is non-quadratic, thus it generally encompasses local minima besides the desired global minimum. For such reason current implementations of FWI rely on initial models that are close to the global minimum. FWI is popularly implemented using the non-linear conjugate gradient method and the Newton-Raphson method.

Meanwhile, linearized waveform inversion consists of realizations of the wave equation keeping the background model, $\mathbf{m}_0 = \mathbf{b}_0 + \mathbf{\Delta b} + \mathbf{r}_0$, unchanged. We only invert for the perturbation of the reflectivity, $\mathbf{\Delta r}$, employing the Born approximation (Barnier and Almomin, 2014). We usually linearize the modeling operator around $\mathbf{r}_0 = 0$ by smoothing the background model (Barnier and Almomin, 2014). Such assumption of smooth background model typically corresponds to attenuation or removal of direct arrivals and diving waves applied to the recorded data. Thus, the LWI misfit function is giving as

$$\Phi_{LWI}(\mathbf{m}) = \| L(\mathbf{m}_0)\mathbf{\Delta r} - \left[\mathbf{d}_r - \pounds(\mathbf{m}_0)\right] \|_2^2 \tag{5}$$

where $\pounds(\mathbf{m}_0)$ constitutes the modeled data obtined using the background model, $\mathbf{m}_0$, thus containing no reflections but direct arrivals and diving waves to be subtracted from the recorded data, $\mathbf{d}_r$ (in practice, "surgical" filters are designed to remove such seismic events). $L(\mathbf{m}_0)\mathbf{\Delta r}$ constitutes the Born modeling operator, defined as

$$L(\mathbf{m}_0)\mathbf{\Delta r}(\mathbf{x},t) : \begin{cases} \left[\mathbf{m}_0\dfrac{\partial^2}{\partial t^2} - \nabla^2\right]\mathbf{u}_0(\mathbf{x},t) = \mathbf{s}(\mathbf{x},t) \\ \left[\mathbf{m}_0\dfrac{\partial^2}{\partial t^2} - \nabla^2\right]\mathbf{u}(\mathbf{x},t) = \mathbf{\Delta r}(\mathbf{x},t)\dfrac{\partial^2\mathbf{u}_0(\mathbf{x},t)}{\partial t^2} \\ \mathbf{d}(\mathbf{x}_r,t) = \mathbf{u}(\mathbf{x}=\mathbf{x}_r,t) \end{cases} \tag{6}$$

In the first term of Equation 6 we obtain the source wavefield, $\mathbf{u}_0$, by solving the acoustic wave equation as in Equation 4, but with the smooth background model, $\mathbf{m}_0$. We then compute in the second term the *scattered wavefield*, $\mathbf{u}$, which is the product of the interaction of the source wavefield with the perturbation in the reflectivity. Finally, we sample the scattered wavefield at the receiver locations. Born operator $L(\mathbf{m}_0)\mathbf{\Delta r}$ is linear respect to the perturbation of the reflectivity, $\mathbf{\Delta r}$, which

constitutes the *seismic image*. This linearity is easy to understand if we recall that the source term of the wave propagation operator is linear respect to the source. In fact, the product $\mathbf{\Delta r}(\mathbf{x},t)\dfrac{\partial^2 \mathbf{u}_0}{\partial t^2}$ constitutes a secondary source term that produces the scattered wavefield, $\mathbf{u}$. The linearity of LWI implies that the misfit function (Equation 5) is quadratic, suggesting that there is a global minimum that potentially could be reached, applying iterative solvers like steepest descent and conjugate gradient. In practice, the huge volumes of typical seismic data make too expensive go beyond a couple of tens iterations. Even if we could afford more iterations, noise in the data and the existance of model and data null spaces would prevent significant progress.

Going back to our proposal, the premise behind LWI with velocity update comes from the fact that the full FWI Hessian can be represented as the sum of two components (Biondi et al., 2015): the Gauss-Newton Hessian, $\mathbf{H}_{GN}$, and the "wave-equation migration velocity analysis" (WEMVA) Hessian, $\mathbf{H}_W$, or simply WEMVA operator, $\mathbf{W}$. The Gauss-Newton Hessian constitutes the product of the so-called Jacobian matrix by its adjoint. In the general case the Jacobian matrix, $\mathbf{J}(\mathbf{m})$, for a generic model, $\mathbf{m}$, is obtained by deriving the synthetic wavefield respect to the model parameters and evaluating at the current model:

$$\mathbf{J}(\mathbf{m}_{curr}) = \frac{\partial \mathbf{u}(\mathbf{m})}{\partial \mathbf{m}}\Big|_{\mathbf{m}=\mathbf{m}_{curr}}, \tag{7}$$

where the synthetic wavefield, $\mathbf{u}(\mathbf{m})$, corresponds either to full wave propagation or Born approximation (Equations 4 and 6, respectively). In the case of LWI, from Equation 5 the Jacobian is given as

$$\mathbf{J}(\mathbf{m} = \mathbf{\Delta r}) = \mathbf{L}, \tag{8}$$

where $\mathbf{L}$ is the matrix representation of the linear Born modeling operator, $L(\mathbf{m})$. Hence, the corresponding Gaussian-Newton Hessian is given as

$$\mathbf{H}_{GN} = \mathbf{L}^T\mathbf{L}, \tag{9}$$

The WEMVA part of the Hessian, $\mathbf{W}$, it is only applicable to FWI because requires the second derivative of the synthetic wavefield respect to the model parameters, which is clearly zero in the case of LWI. This operator is composed of two parts (Biondi et al., 2015): the source side, $\mathbf{W}_s$, which is given by the correlation of the source wavefield with the receiver scattered wavefield, and the receiver side, $\mathbf{W}_r$, which is the correlation of the receiver wavefield with the source scattered wavefield. The term *scattered wavefield* refers to the interaction of the corresponding wavefields with an image or model perturbation. The main difference of conventional WEMVA respect to FWI related WEMVA is that in the latter, both the receiver wavefield and the receiver scattered wavefield are applied to the data residuals ($\mathbf{\Delta d} = \mathbf{d}_m - \mathbf{d}_r$) instead to the recorded data, $\mathbf{d}_r$.

So far, current implementations of LWI work exclusively with the corresponding Gauss-Newton Hessian (Equation 9). We propose to include model (velocity) updates

in the process, basing upon the incorporation of the WEMVA Hessian to the conventional LWI misfit function (Equation 5). In this report we do not consider another possible alternative: begin with the FWI misfit function (Equation 3) and simplify from there. Such possibility is a topic for future research.

ALGORITHM PROPOSED

In this section we present an algorithm conceived to perform LWI updating the reflectivity model, $\mathbf{\Delta r}$, per usual, but allowing a controlled variation of the background model, $\mathbf{\Delta b}$.

Let us consider the following optimization problem:

$$\Phi(\mathbf{\Delta r}, \mathbf{\Delta b}; \mathbf{b}_0) = \frac{1}{2}\|\mathbf{H}_{GN}(\mathbf{b}_0)\mathbf{\Delta r}+\mathbf{H}_W(\mathbf{b}_0)\mathbf{\Delta b}-\mathbf{\Delta r}_{mig}\|_2^2-\frac{\lambda}{2}[\mathbf{H}_W(\mathbf{b}_0)\mathbf{\Delta b}+\mathbf{\Delta r}_{mig}]^2. \tag{10}$$

Here, $\mathbf{\Delta r}_{mig}$ represents the image obtained by conventional RTM. Equation 10 is interpreted as the search for the optimal perturbation of reflectivity ($\mathbf{\Delta r}$) and perturbation in the background slowness ($\mathbf{\Delta b}$), given a seismic experiment realization performed on an acoustic medium of spatially variable, but fixed smooth background slowness, $\mathbf{b}_0$. The resulting reflectivity obtained from $\mathbf{H}_{GN}\mathbf{\Delta r} + \mathbf{H}_W\mathbf{\Delta b}$ is expected to fit the conventionally RTM migrated image (first term of the righthand side). Such optimization is subject to the condition that the perturbation in the image contributed by $\mathbf{H}_W\mathbf{\Delta b}$, when added to the migrated image, yields a maximum in terms of stacking power (second term). The minus sign signifies that we perform the maximization of stacking power by minimizing negative value of the function. We control this constraint with the parameter λ.

Let us simplify Equation 10 by dropping the explicit dependence on $\mathbf{b}_0$, and substitute $\mathbf{W}$ for $\mathbf{H}_W$:

$$\Phi(\mathbf{\Delta r}, \mathbf{\Delta b}) = \frac{1}{2}\|\mathbf{H}_{GN}\mathbf{\Delta r} + \mathbf{W}\mathbf{\Delta b} - \mathbf{\Delta r}_{mig}\|_2^2 - \frac{\lambda}{2}\|\mathbf{W}\mathbf{\Delta b} + \mathbf{\Delta r}_{mig}\|^2. \tag{11}$$

In the first term we can express the Hessian components as a matrix product,

$$\Phi(\mathbf{\Delta r}, \mathbf{\Delta b}) = \frac{1}{2}\| \begin{bmatrix}\mathbf{H}_{GN} & \mathbf{W}\end{bmatrix} \begin{bmatrix}\mathbf{\Delta r} \\ \mathbf{\Delta b}\end{bmatrix} - \mathbf{\Delta r}_{mig}\|_2^2 - \frac{\lambda}{2}[\mathbf{W}\mathbf{\Delta b} + \mathbf{\Delta r}_{mig}]^2. \tag{12}$$

The corresponding fitting functions (Claerbout, 2014) are

$$\begin{bmatrix}\mathbf{H}_{GN} & \mathbf{W}\end{bmatrix} \begin{bmatrix}\mathbf{\Delta r} \\ \mathbf{\Delta b}\end{bmatrix} - \mathbf{\Delta r}_{mig} \approx \mathbf{0}$$
$$-\lambda\mathbf{W}\mathbf{\Delta b} - \lambda\mathbf{\Delta r}_{mig} \approx \mathbf{0}$$

We can re-cast the fitting functions as a matrix operation,

$$\begin{bmatrix}\mathbf{H}_{GN} & \mathbf{W} \\ \mathbf{0} & -\lambda\mathbf{W}\end{bmatrix} \begin{bmatrix}\mathbf{\Delta r} \\ \mathbf{\Delta b}\end{bmatrix} = \begin{bmatrix}\mathbf{\Delta r}_{mig} \\ \lambda\mathbf{\Delta r}_{mig}\end{bmatrix}, \tag{13}$$

which defines our forward modeling operator. The corresponding adjoint operator is defined by taking the transpose of the big matrix in Equation 13,

$$\begin{bmatrix} \Delta\tilde{\mathbf{r}} \\ \Delta\tilde{\mathbf{b}} \end{bmatrix} = \begin{bmatrix} \mathbf{H}_{GN}^T & \mathbf{0} \\ \mathbf{W}^T & -\lambda\mathbf{W}^T \end{bmatrix} \begin{bmatrix} \Delta\mathbf{r}_{mig} \\ \lambda\Delta\mathbf{r}_{mig} \end{bmatrix}. \tag{14}$$

Now $[\Delta\tilde{\mathbf{r}} \quad \Delta\tilde{\mathbf{b}}]^T$ constitutes the first estimation of the perturbations in reflectivity and background model. Equations 13 and 14 constitute the elements to set an iterative solution scheme, such as linear conjugate gradients, to solve LWI with velocity updates.

DISCUSSION: IMPLEMENTATION AND FUTURE WORK

Figure 1 shows a flowchart with the implementation of LWI with velocity updates using the conjugate gradient method. The objective is to analyze which elements can be possibly recycle or precomputed, and which ones have to be computed "on the fly".

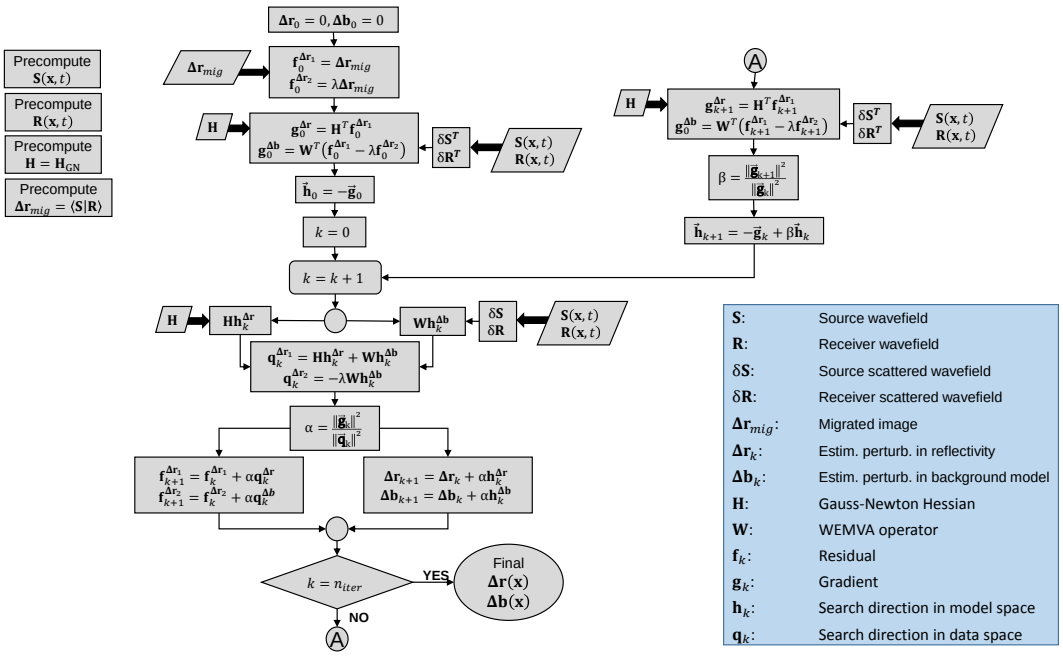

Figure 1: Flowchart of the conjugate gradient method applied to LWI with velocity updates

ACKNOWLEDGEMENTS

We would like to thank the SEP sponsors for their support. Alejandro Cabrales would like to thank Petroleos Mexicanos for the financial support.

REFERENCES

Araujo, E., R. Pestana, and A. dos Santos, 2014, Symplectic scheme and the Poynting vector in reverse-time migration: Geophysics, **79**, no. 5, S163–S172.

Barnier, G. and A. Almomin, 2014, Tutorial on two-way wave equation operators for acoustic, isotropic, constant-density media: SEP-Report, **155**, 23–56.

Baysal, E., D. Kosloff, and J. Sherwood, 1983, Reverse time migration: Geophysics, **48**, 1514–1524.

Biondi, B., 2002, Stable wide-angle fourier finite-difference downward extrapolation of 3-D wavefields: Geophysics, **67**, 872–882.

Biondi, B., E. Biondi, M. Maharramov, and Y. Ma, 2015, Dissection of the full-waveform inversion hessian: SEP-Report, **160**, 19–38.

Claerbout, J., 1971, Toward a unified theory of reflector mapping: Geophysics, **36**, 467–481.

Claerbout, J. F., 2014, Geophysical image estimation by example: Jon Claerbout.

Dai, W., C. Boonyasiriwat, and G. Schuster, 2010, 3D Multi-source Least-squares Reverse Time Migration: SEG Technical Program Expanded Abstracts, 3120–3124.

Dai, W., Y. Huang, and G. Schuster, 2013, Least-squares reverse time migration of marine data with frequency-selection encoding: SEG Technical Program Expanded Abstracts, 3231–3236.

Douma, H., D. Yingst, I. Vasconcelos, and J. Tromp, 2010, On the connection between artifact filtering in reverse-time migration and adjoint tomography: Geophysics, **75**, no. 6, S219–S223.

Duquet, B., K. Marfurt, and J. Dellinger, 2000, Kirchhoff modeling, inversion for reflectivity, and subsurface illumination: Geophysics, **65**, 1195–1209.

Gazdag, J. and E. Carrizo, 1986, On reverse-time migration: Geophysical Prospecting, **34**, 822–832.

Hestenes, M. and E. Stiefel, 1952, Methods of conjugate gradients for solving linear systems: Journal of Research of the National Bureau of Standards, **49**, no. 6, 409–436.

Ji, J., 1992, Reverse-time migration as the conjugate of forward modeling: SEP-Report, **75**, 135–143.

———, 2009, An exact adjoint operation pair in time extrapolation and its application in least-squares reverse-time migration: Geophysics, **74**, no. 5, H27–H33.

Jiang, Z. and S. Schuster, 2003, Target-oriented least squares migration: SEG Technical Program Expanded Abstracts, 1043–1046.

Kosloff, D. and E. Baysal, 1983, Migration with the full acoustic wave equation: Geophysics, **48**, 677–687.

Liu, F., Z. Guanquan, S. Morton, and J. Leveille, 2011a, An effective imaging condition for reverse-time migration using wavefield decomposition: Geophysics, **76**, no. 1, S29–S39.

Liu, Y., X. Chang, R. Jin, R. He, and Z. Y. Sun, H., 2011b, Reverse time migration of multiples for subsalt imaging: Geophysics, **76**, no. 5, WB209–WB216.

Liu, Y., H. Hu, X. Xie, Y. Zheng, and P. Li, 2015, Reverse time migration of internal multiples for subsalt imaging: Geophysics, **80**, no. 5, S175–S185.

McMechan, G., 1983, Migration by extrapolation of time-dependent boundary values: Geophysical Prospecting, **31**, 413–420.

Nemeth, T., C. Wu, and G. Schuster, 1999, Least-squares migration of incomplete reflection data: Geophysics, **64**, 208–221.

Ren, L., Liu, X. G., Meng, J. Wang, and S. Zhang, 2013, Suppressing artifacts in 2D RTM using the Poynting vector: SEG Global Meeting Abstracts, 484–487.

Ristow, D. and T. Rühl, 1994, Fourier finite-difference migration: Geophysics, **59**, 1882–1893.

Rocha, D., N. Tanushev, and P. Sava, 2015a, Acoustic wavefield imaging using the energy norm: SEG Technical Program Expanded Abstracts, 4085–4090.

———, 2015b, Elastic wavefield imaging using the energy norm: SEG Technical Program Expanded Abstracts, 2124–2128.

Ronen, S. and C. Liner, 2000, Least-squares DMO and migration: Geophysics, **65**, 1364–1371.

Stoffa, P., J. Fokkema, de Luna Freire R., and W. Kessinger, 1990, Split-step fourier migration: Geophysics, **56**, 410–421.

Wong, M., B. Biondi, and S. Ronen, 2015, Imaging with primaries and free-surface multiples by joint least-squares reverse time migration: Geophysics, **80**, no. 6, S223–S235.

Wong, M., S. Ronen, and B. Biondi, 2011, Least-squares reverse time migration/inversion for ocean bottom data: a case study: SEG Technical Program Expanded Abstracts, 2369–2373.

Yoon, K. and K. Marfurt, 2006, Reverse-time migration using the Poynting vector: Exploration Geophysics, **37**, 102–107.

Zhan, Y., L. Duan, and Y. Xie, 2015, A stable and practical implementation of least-squares reverse time migration: Geophysics, **80**, no. 1, V23–V31.